Available online at www.sciencedirect.com

ScienceDirect

Nuclear and Particle Physics Proceedings 273–275 (2016) 361–366

www.elsevier.com/locate/nppp

Direct Dark Matter Search with XMASS

Kazuyoshi Kobayashi[ab] for the XMASS collaboration

[a] *Kamioka observatory, Institue for Cosmic Ray Research, the University of Tokyo, Higashi-Mozumi, Kamioka, Hida, Gifu, 506-1205, Japan*
[b] *Kavli Institute for the Physics and Mathematics of the Universe (WPI), the University of Tokyo, Kashiwa, Chiba, 277-8582, Japan*

Abstract

The purpose of current XMASS project is dark matter detection. With 835 kg liquid xenon, we searched for various kinds of dark matter candidate using commissioning data. In order to reduce the background contribution from the PMT surface material, we have refurbished the detector and restarted to take data in November, 2013. Future project of XMASS is also shown.

Keywords: Dark matter, WIMP, Xenon

1. Introduction

The XMASS project aims at detecting dark matter, pp and ^{7}Be solar neutrinos, and neutrino less double beta decay using large volume of pure liquid xenon. The original idea is presented in Ref. [1]. The first physics target of the XMASS experiment is to detect dark matter. Various astronomical observations [2] provide strong evidence for a large amount of dark matter in the universe. However, its nature is still unknown. Weakly interacting massive particles (WIMPs) are dark matter candidates motivated by theories beyond the Standard Model [3]. This project searches for nuclear recoils in liquid xenon caused by WIMPs. Since XMASS is sensitive not only to nuclear recoils but also electron recoils, various candidates of dark matter are also searched for. In the commissioning run, we found major background coming from the PMT part. To minimize the background contribution, detector refurbishment (RFB) are performed. Future prospect are also shown.

2. XMASS detector

The XMASS detector is located in the Kamioka mine 1000m underneath the top of Mt. Ikenoyama (i.e. 2700 m water equivalent underground) in Japan. The detector consists of two components, the inner and outer detectors (ID and OD, respectively).

The ID is equipped with 642 inward-facing photomultiplier tubes (PMTs) in an approximate spherical shape in a copper vessel filled with pure liquid xenon. Six hundred and thirty hexagonal PMTs (HAMAMATSU R10789-11) and twelve round PMTs (HAMAMATSU R10789-11MOD) are mounted in an oxygen free high conductivity (OFHC) copper holder with an approximately spherical shape called a pentakis-dodecahedron. The shape of the pentakis-dodecahedron consists of 60 isosceles triangles. One triangular module holds approximately 10 PMTs. The entire structure is immersed in liquid xenon. The amount of liquid xenon in the sensitive region is 835 kg. The PMT photo coverage of more than 62% is achieved and the PMT quantum efficiency at the scintillation wavelength of liquid xenon (~175 nm) is more than 28%. The vessel which holds liquid xenon and the PMT holder is made of OFHC copper and the size is 1120 mm in diameter. To reduce the amount of liquid xenon, an OFHC copper filler is installed in the gap between the PMT holder and the inner vessel. The vessel is covered with another vessel for vacuum insulation.

http://dx.doi.org/10.1016/j.nuclphysbps.2015.09.051

The ID is installed at the centre of the OD, which is a cylindrical water tank with seventy two 20-in. PMTs. The OD is used as an active shield for cosmic ray muons and a passive shield for low-energy gamma rays and neutrons. Construction of the detector started in April 2007 and was completed in September 2010. Commissioning runs were conducted from October 2010 to June 2012. Since the detector structure around the PMT surface was changed, the detector before refurbishment is called XMASS-I.

3. Physics results from XMASS-I

In the commissioning run, we took data under various kinds of condition in order to understand the detector. However, using the data under stable condition, we performed the physics analysis searching for various dark matter candidates

3.1. Light WIMP search

Possible light WIMP signals with a mass of ~10 GeV are indicated by some experiments [5] around the spin-independent cross section of the order of $\sim 10^{-40}$ cm^2. These positive signals have come predominantly from experiments without discrimination of nuclear recoil signals from that of electromagnetic, while other experiments [6] that have this ability have excluded light WIMPs at these cross sections. XMASS is capable to search for light WIMP signals with low (0.3 keV) threshold because of our exceptional photoelectron yield, which is the largest among current low background detectors. We searched for the light WIMP signals without nuclear recoil discrimination. The data with 6.70 days livetime taken in February 2012 is used for this analysis.

Standard data reduction is applied to remove non-scintillation light events, mainly. The standard data reduction consists of a series of cuts: (1) the event is triggered only by the ID; (2) the time difference to the previous event is more than 10 ms; (3) the root mean square of the hit timing is less than 100 ns; and (4) the number of PMT hits in the first 20 ns divided by the total number of hits is less than 0.6 for events in which the number of photoelectrons is less than 200. The second and third cuts are applied to remove PMT after pulses due to bright events and electronic ringing. The fourth cut is applied to remove Cherenkov events originated from ^{40}K in photo cathodes (Cherenkov cut).

Fig.1 shows the scaled energy distribution after the data reduction compared with Monte Carlo simulations. Since the 5.9 keV X-ray from ^{55}Fe is the lowest energy calibration point, the response at lower energies is extrapolated using a linear fit using all calibration energies. The fitting error from this procedure, 1.3% at 0.3 keV, is treated as a systematic effect on the energy scale. However, the effect of this uncertainty is small relative to that induced by the uncertainty in L_{eff}, which is 13% at the same energy. WIMPs are assumed to be distributed in an isothermal halo with v_o = 220 km/s, a galactic escape velocity of v_{esc} = 650 km/s, and an average density of 0.3 GeV/cm^3. In order to set a conservative upper bound on the spin-independent WIMP-nucleon cross section, the cross section is adjusted until the expected event rate in XMASS does not exceed the observed one in any energy bin above 0.3 keV. The 90% confidence level (C.L.) limit derived is shown in Fig. 2. The detail result is shown in Ref. [7].

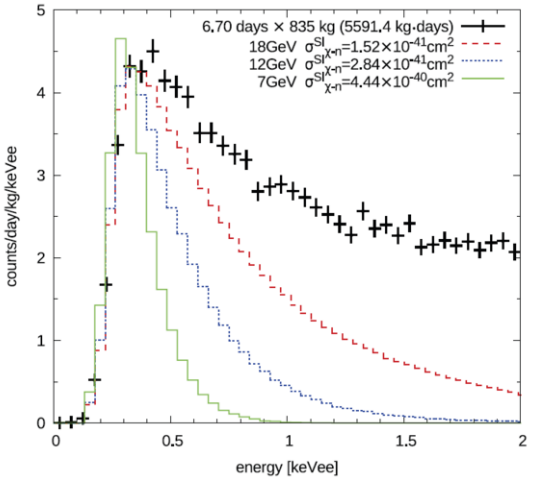

Fig.1. Observed scaled energy spectrum compared with that of simulation with 7 GeV, 12GeV, and 18GeV WIMP masses.

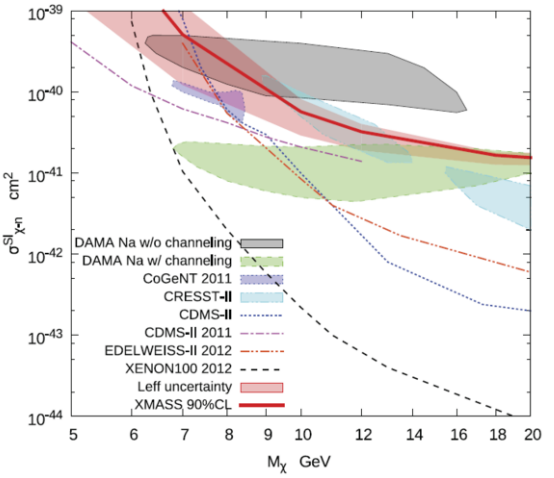

Fig.2. Upper limit at 90% C.L. on spin independent elastic WIMP cross section compared with other experiments.

3.2. Solar axions search

The axion is a hypothetical particle postulated for solving the CP problem in strong interactions. The DFSZ axions [8] have direct couplings to leptons though the KSVZ axions (hadronic axions) [9] do not have tree-level couplings to leptons. We searched for axions as well as axion-like particles (ALPs) focusing on couplings to electrons (g_{aee}). Although experimental searches that utilize coupling to photons ($g_{a\gamma\gamma}$) successfully improved sensitivities, an efficient experimental search with g_{aee} has not been performed. A pioneering experiment used a Ge detector [10] and a recent search used a Si (Li) detector to search for signals from axions generated by the bremsstrahlung and Compton effect via the axioelectric effect. The signals we searched for are produced by the Compton scattering of photons on electrons $e+\gamma \rightarrow e+a$ and the bremsstrahlung of axions from electrons $e+Z \rightarrow e+a+Z$ in the Sun. The dataset and data reduction used for this analysis is same as light WIMP search. The observed spectra shown in Fig. 3 do not have any significant excesses to identify axion signals. Strong constraints on g_{aee} can be obtained from the observed event rate in the relevant energy range. In order to set a conservative upper limit on the axion-electron coupling constant g_{aee}, the coupling is adjusted until the expected event rate does not exceed the one observed in any energy bin above 0.3 keV. Fig.4 shows the upper limit on g_{aee}. For small axion masses, a g_{aee} of 5.4×10^{-11} is obtained. This was the best direct experimental limit to date and is close to that derived from astrophysical considerations based on measured solar neutrino fluxes g_{aee} =2.8×10^{-11}. The detail is shown in Ref. [11].

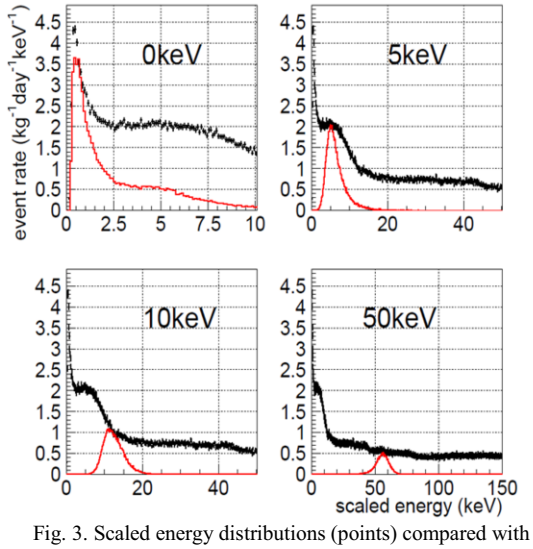

Fig. 3. Scaled energy distributions (points) compared with axion simulations (histogram) with 0, 5, 10, and 50 keV axion masses.

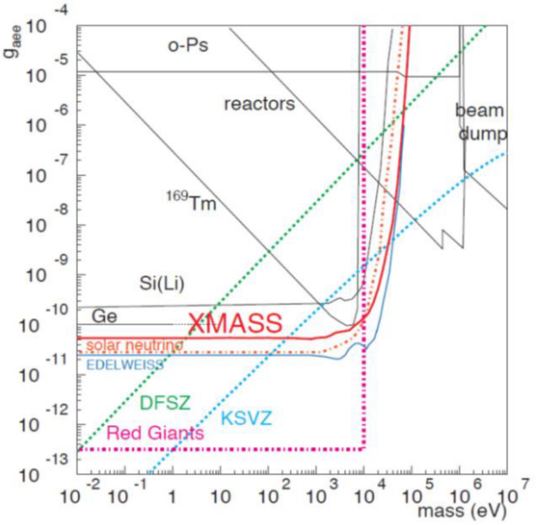

Fig. 4. Upper limit on g_{aee} as a function of axion mass compared with limits from other experiments and astrophysical observabtions.

3.3. Inelastic WIMP nucleus scattering search

Although many experiments has been searched for WIMP signal using WIMP-nucleus elastic scattering, the inelastic scattering can also be searched for using the de-excitation signal from the excited nucleus. The advantage of the search for inelastic scattering is that the de-excitation signal is much more energetic than that of elastic scattering and its process is typically well studied. Among the xenon isotopes found in naturally abundant xenon, ^{129}Xe has the lowest-lying excited nuclear state at 39.58 keV with 26.4% abundance which is highest. The second highest nucleus would be ^{131}Xe with 21.2% abundance and with an 80.19 keV excitation. The DAMA experiment has searched for the signal in a 2500 kg day exposure of 6.5 kg of LXe. They used 99.5% enriched ^{129}Xe and constrained the inelastic cross section for 50 GeV WIMPs to be less than 3 pb at the 90% C.L. [12].

The data used in this analysis is taken between December 2010 and May 2012. Total livetime is estimated to be 165.9 days. After applying standard data reduction which is described in light WIMP search, the following cuts are applied in addition: (1) Fiducial volume cut. The events remain if reconstructed radius position R is less than 15 cm. (2) Timing cut. (3) Band cut. The first and second cuts are applied to remove surface background events. The third cut is applied to remove events occurring at the grooves and gaps between PMTs. These events make band pattern in hit structure and are identified using the hit pattern and removed. As shown in Fig. 5, these

cuts eliminate most of all background in and around the signal window. After all cuts, 5 events remain in our 36-48 keV signal region. However, we don't see any significant excesses above the background. The main contribution to the remaining background comes from the ^{222}Rn daughter ^{214}Pb. From our simulation we estimate this background alone to contribute 2.0 ± 0.6 events. As other background contributions are smaller but less certain, we do not subtract background for obtaining our limits. Derived 90% C.L. upper limit for this cross section is shown in Fig. 6. The gray band reflects our systematic uncertainties. It should be noted that the constraint obtained by the DAMA experiment [12] was derived from a statistical evaluation of an excess above a large background of 2×10^{-2} keV^{-1} day^{-1} kg^{-1}. We achieved a significantly lower background ~ 3×10^{-4} keV^{-1}day^{-1} kg^{-1} using the cut discussed above. The detail is shown in Ref. [13].

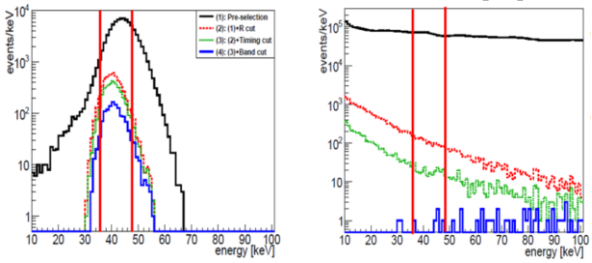

Fig. 5. Scaled energy distributions in each reduction step (right: WIMP signal simulation with a mass of 50 GeV, left: data).

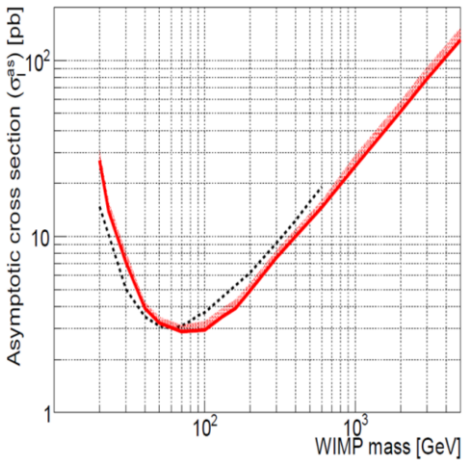

Fig. 6. Upper limit on cross section for inelastic scattering on ^{129}Xe at 90% C.L.. Dotted line shows the limit obtained from the DAMA experiment.

3.4. Bosonic super-WIMPs search

Lighter and more weakly interacting particles such as super-WIMPs are warm dark matter candidates [14]. If the mass of the super-WIMPs is above ~3 keV, there is no conflict with structure formation in the Universe [15]. Bosonic super-WIMPs are experimentally interesting since their absorption in a target material would deposit an energy essentially equivalent to the super-WIMP's rest mass.

The same data set as inelastic WIMP nucleus scattering search is used for this analysis. The event selections are also similar, but parameters are optimized for this analysis. As shown in Fig. 7, no siginificant excesses in the signal region are found. Fig. 8 shows the obtained limit on the coupling constat at 90% C.L.. This is the first direct search for vector bosonic super-WIMPs in this mass range. It cannot explained that such WIMPs constitute all the dark matter from this result. The detail is shown in Ref. [16].

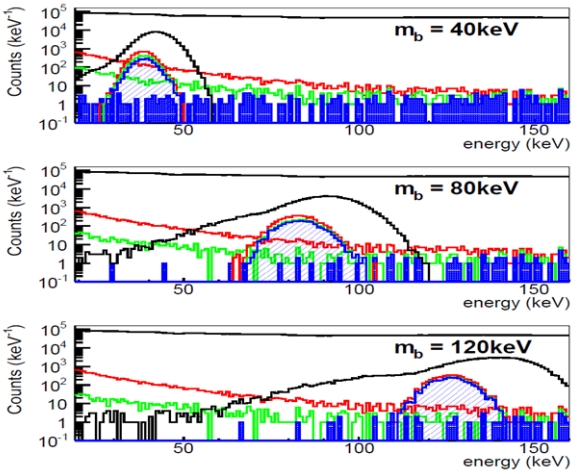

Fig. 7 Scaled energy distributions. Data shows continuous distributions in each reduction step with optimized cut for 40, 80, 120 keV vector boson masses. Distributions with bump show signal simulations.

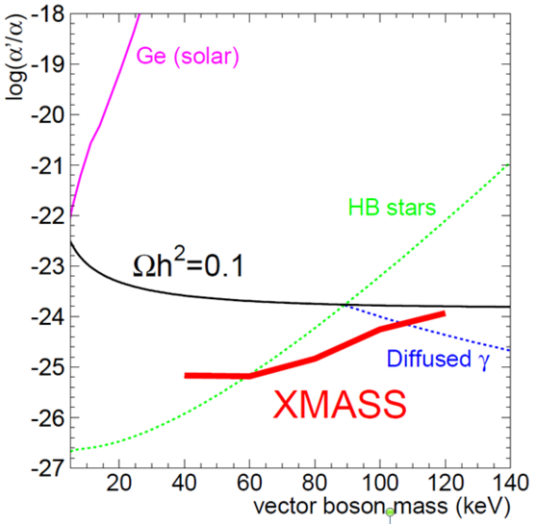

Fig. 8. Limit on coupling constants for vector bosons. The thin solid line shows the expected coupling constant required to explain the observed dark matter abundance.

4. Detector refurbishment

During the commissioning run, detail study for background was performed. Then we found that the main background comes from the aluminium sealing material at PMT photocathode. To minimize the background contribution from the sealing material, it is covered with copper ring as shown in Fig. 9 and also high purity aluminium is evaporated around it. In addition, since the background from grooves and gaps can mimic the dark matter signal, electro-polished copper plates were put on the surface as shown in Fig. 10. The detector RFB has finished and we have started data taking in November 2014. The event rate after standard data reduction above 5 keV became lower by one order of magnitude. We are now analyzing the data in detail. We have already taken more than 120 days of data and plans to take more than one year of data.

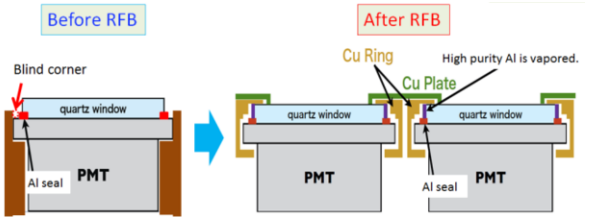

Fig.9. Schematic view of the PMT cover before and after RFB.

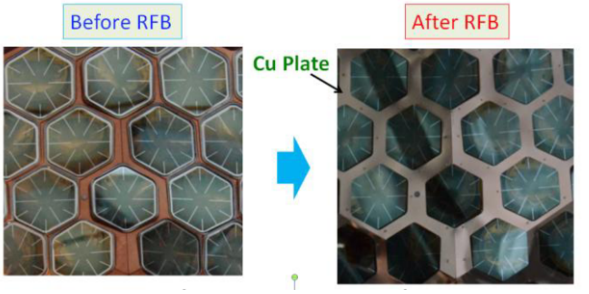

Fig.10. Photos of ID surface before and after RFB. Copper plates are installed on the surface of detector to reduce the grooves and gaps between PMTs.

5. Future prospect

We are planning to make a ton scale fiducial volume (5 tons in full volume) detector, XMASS 1.5. The detector structure of XMASS 1.5 is basically similar to the current one. However, the largest difference is the PMT. We plan to use low background aluminium and also the round shape of PMT photocathode, which is sensitive to the light emitted around the side of PMT. It would help to reduce the surface background. The target sensitivity is ~10^{-46} cm^2 for 100 GeV WIMP as shown in Fig. 11.

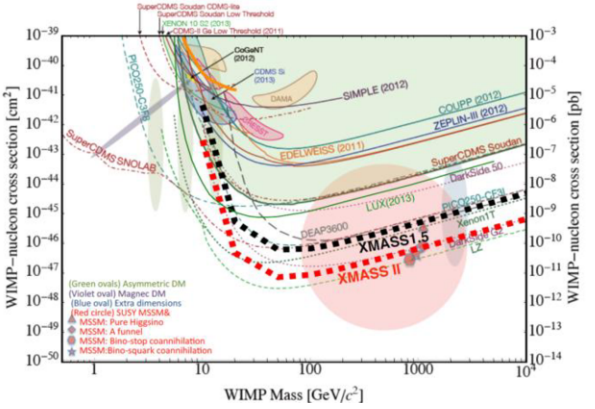

Fig.11. Sensitivity of XMASS 1.5 and XMASS II.

.

References

[1] Y. Suzuki, arXiv:hep-ph/0008296.
[2] K.G. Begeman, A.H. Broeils, R.H. Sanders, Monthly Notices of the Royal Astron. Soc. 249 (1991) 523; J. Dunkley, et al., Astrophysical Journal Supplement 180 (2009) 306; R.A. Knop, et al., Astrophysical Journal 598 (2003) 102; S.W. Allen, et al., Monthly Notices of the Royal Astron. Soc. 334 (2002) L11; M. Tegmark, et al., Phys. Rev. D 69 (2004) 103501.

[3] H.C. Cheng, et al., Phys. Rev. Lett. 89 (2002) 211301; A. Birkedal-Hansen, J.G. Wacker, Phys. Rev. D 69 (2004) 065022; A. Bottino, et al., Phys. Rev. D 69 (2004) 037302; J. Ellis, et al., Phys. Rev. D 71 (2005) 095007
[4] K.Abe *et al*, Nucl. Instrum. Methods A 706, 78 (2013).
[5] R. Bernabei, et al., Eur. Phys. J. C 56 (2008) 333; R. Bernabei, et al., Eur. Phys. J. C 67 (2010) 39; C.E. Aalseth, et al., Phys. Rev. Lett. 106 (2011) 131301; G. Angloher, et al., Eur. Phys. J. C 72 (2012) 1971.
[6] E. Aprile, et al., arXiv:1207.5988; J. Angle, et al., Phys. Rev. Lett. 107 (2011) 051301; Z. Ahmed, et al., Science 327 (2010) 1619; Z. Ahmed, et al., Phys. Rev. Lett. 106 (2011) 131302; E. Armengaud, et al., Phys. Rev. D 86 (2012) 051701.
[7] K.Abe *et al*, Phys. Lett. B 719, 78 (2013).
[8] M.Dine, W.Fischler, M.Srednicki, Phys. Lett. B104 (1981) 199; A.R.Zhitnitsky, Sov. J. Nucl. Phys. 31 (1980) 260; A.R.Zhitnitsky, Yad. Fiz. 31 (1980) 497.
[9] J.E.Kim, Phys. Rev. Lett. 43 (1979) 103; M.A.Shifman, A.I.Vainshtein, V.I.Zakharov, Nucl. Phys. B166 (1980) 493.
[10] F.T.Avignone, R.L.Brodzinski, S.Dimopoulos, G.D.Starkman, A.K.Drukier, D.N.Spergel, G.Gelmini, B.W.Lynn, Phys. Rev. D35 (1987) 2752.
[11] K.Abe *et al*, Phys. Lett. B 724, 46 (2013).
[12] P. Belli et al., Phys. Lett. B 387, 222 (1996); R. Bernabei et al., New J. Phys. 2, 15 (2000).
[13] H.Uchida *et al*, Prog.Theor.Exp.Phys. 063C01(2014).
[14] M. Pospelov, A. Ritz, and M. Voloshin, Phys. Rev. D 78, 115012 (2008). J. Redondo and M. Postma, J. Cosmol. Astropart. Phys. 02 (2009) 005.
[15] K. Markovič and M. Viel, Pub. Astron. Soc. Aust. 31, e006 (2014).
[16] K.Abe *et al*, Phys. Rev. Lett. 113, 121301 (2014).